International Journal of the Physical Sciences Vol. 5(5), pp. 564-575, May 2010
Available online at http://www.academicjournals.org/IJPS
ISSN 1992 - 1950 © 2010 Academic Journals

Full Length Research Paper

Mesogenic Schiff base esters with terminal chloro group: Synthesis, thermotropic properties and X-ray diffraction studies

Sie-Tiong Ha[1]*, Lay-Khoon Ong[2], Yasodha Sivasothy[3], Guan-Yeow Yeap[4], Hong-Cheu Lin[5], Siew-Ling Lee[6], Peng-Lim Boey[4] and Nilesh L. Bonde[7]

[1]Department of Chemical Science, Faculty of Science, Universiti Tunku Abdul Rahman, Jln Universiti, Bandar Barat, 31900 Kampar, Perak, Malaysia.
[2]Department of Science, Faculty of Engineering and Science, Universiti Tunku Abdul Rahman, Jln Genting Klang, Setapak, 53300 Kuala Lumpur, Malaysia.
[3]Chemistry Department, Faculty of Science, Universiti Malaya, 50603, Kuala Lumpur, Malaysia.
[4]Liquid Crystal Research Laboratory, School of Chemical Sciences, Universiti Sains Malaysia, 11800 Minden, Penang, Malaysia.
[5]Department of Material Science and Engineering, National Chiao-Tung University, 1001 Ta-Hsueh Road, Hsinchu 300, Taiwan, Republic of China.
[6]Ibnu Sina Institute for Fundamental Science Studies, Universiti Teknologi Malaysia, 81310 UTM Skudai, Johor, Malaysia.
[7]Sterling Biotech Limited, Jambusar State Highway, Village Masar, Tal: Padra, District Vadodara, India.

Accepted 15 April, 2010

A new homologous series of Schiff base esters comprising a terminal chloro substituent was studied. The chloro substituent contributes to the molecular polarizability, thus, affecting intermolecular interactions, hence, resulting in smectic polymorphism. The mesomorphic properties were studied using differential scanning calorimetry, polarizing optical microscopy and temperature-dependent X-ray diffractometry. Whilst the *n*-pentanoyloxy and *n*-heptanoyloxy derivatives exhibited enantiotropic smectogenic A and B phases, monotropic smectogenic A and B phases were observed in the *n*-butanoyloxy and *n*-hexanoyloxy derivatives. Enantiotropic smectogenic A and monotropic smectogenic B phases were observed in the *n*-octanoyloxy to *n*-hexadecanoyloxy derivatives. The highest member of this series, the *n*-octadecanoyloxy derivative, exhibited an enantiotropic smectogen A phase. The homologous members were compared with structurally related series to establish their chemical structure-mesomorphic behavior relationships.

Key words: Schiff base ester, thermotropic properties, smectic A, smectic B, X-ray diffraction.

INTRODUCTION

The development of liquid crystal science and technology has led to the preparation and study of numerous mesogens in particular, thermotropic liquid crystals (Yuksel et al., 2007; Zhang et al., 2005). Most thermotropic liquid crystals are rod-like molecules having a rigid core composed of two or more aromatic rings and one or more flexible terminal chains. Schiff base, also known as imine (CH=N), is a linking group used in connecting two core groups. Though it provides a stepped core structure, it maintains molecular linearity, hence providing higher stability and enabling mesophase formation (Collings and Hird, 1998; Singh and Dunmur, 2002). Extensive investigation on Schiff base core systems have been conducted since the discovery of MBBA which exhibited a nematic phase at room temperature (Kelker and Scheurle, 1969). Several studies have been conducted on Schiff base esters owing to their

*Corresponding author. E-mail: hast_utar@yahoo.com, hast@utar.edu.my. Fax: 6054661676.

interesting properties and considerable temperature range (Eran et al., 2008; Ha et al., 2009a, b; Parra et al., 2004; Prajapati and Varia, 2008; Vora et al., 2001; Yeap et al., 2004, 2006a, b, c).

Typical terminal moieties exhibiting liquid crystal properties are those with electronegative atoms, such as halogens. Halogens (F, Cl, Br and I) are polar substituents possessing strong dipole moments, thus having the ability to promote mesomorphic properties (Galewski, 1994; Galewski and Coles, 1999; Sakagami and Nakamizo, 1980). The increased dipole moment enhances the stability of the lattice and melting temperatures (Singh and Dunmur, 2002). Chlorine has a polarisability and size which lies between fluorine and bromine (Yeap et al., 2004; 2006a). As the ionic radius of the terminal substituent increases, the molecules tend to orientate in a parallel arrangement (Dave and Menon, 2000). Thus, smectic polymorphism is not unusual for mesogens with a terminal chloro substituent, and this has been frequently observed as the length of the alkyl or alkoxy chains increases (Galewski and Coles, 1999; Petrov et al., 2001).

As a continuation of our previous work, Schiff base esters and chlorine terminal moieties are incorporated to form a new series of homologous compounds, 4-alkanoyloxybenzylidene -4'-chloroanilines, nClAB. FT-IR, ^{1}H and ^{13}C NMR, EI-MS and elemental analysis were employed to elucidate the molecular structure of the title compounds whereas the liquid crystal properties were determined by DSC, POM and XRD analysis. The mesomorphic behaviors of the homologous compounds are rationalized based on the varying lengths of the alkyl chain. In addition, the relationship between the molecular structure and liquid crystal properties is also discussed in this paper.

MATERIALS AND METHODS

Materials

4-Hydroxybenzaldehyde, 4-chloroaniline, 4-dimethylaminopyridine, acetic acid, butyric acid, hexanoic acid, heptanoic acid, decanoic acid, dodecanoic acid, tetradecanoic acid, hexadecanoic acid and octadecanoic acid were obtained from Merck (Germany) without further purification. Propionic acid, pentanoic acid, octanoic acid and N, N-dicyclohexylcarboiimide was acquired from Acros Organics (USA).

Electron impact mass spectrum (EI-MS) was recorded using a Finnigan MAT95XL-T mass spectrometer operating at 70 eV ionizing energy. Samples were introduced using a direct inlet system with a source temperature of 200°C. Microanalyses were carried out on a Perkin Elmer 2400 LS Series CHNS/O analyser. FT-IR data (Figure 1) were acquired with a Perkin Elmer 2000-FTIR spectrophotometer in the frequency range of 4000 - 400 cm^{-1} with samples embedded in KBr discs. ^{1}H and ^{13}C NMR spectra were recorded in $CDCl_3$ using a JEOL 400MHz NMR Spectrometer with TMS as the internal standard. Thin layer chromatography analyses were carried out using aluminum backed silica gel plates (Merck 60 F_{254}) and were examined under shortwave UV light.

The phase transition temperatures were measured using a Mettler Toledo DSC823 differential scanning calorimeter (DSC) at a scanning rate of 10°Cmin^{-1}. Liquid crystalline properties were investigated by polarizing optical microscopy (POM) using a Carl Zeiss Polarizing Optical Microscope (POM) attached to a Linkam Hotstage. The texture of the compounds were observed using polarized light with crossed polarizers, the sample being prepared as a thin film sandwiched between a glass slide and a cover. A video camera (Video Master coomo20P) was installed on the polarizing microscope and coupled to a video capture card (Video master coomo600), allowing real-time video capture and image saving.

Synchrotron powder X-ray diffraction (XRD) measurements were performed at beamline BL17A where the X-ray wavelength used was 1.32633 Å. The XRD data were collected using imaging plates (IP, of an area = 20 × 40 cm^2 and a pixel resolution of 100) curved with a radius equivalent to the sample-to-image plate distance of 280 mm, and the diffraction signals were accumulated for 3 min. The powder samples were packed into a capillary tube and heated by a heat gun, where the temperature controller was programmed by a PC with a PID feedback system. The scattering angle theta was calibrated by a mixture of silver behenate and silicon.

Synthesis

The intermediate and title compounds were prepared according to previously reported methods (Ha et al., 2009a, b).

Synthesis of 4-hydroxybenzylidene- 4'-chloroaniline, ClHAB

Equal amounts of 4-hydroxybenzaldehyde and 4-chloroaniline, along with three drops of acetic acid and 30 mL of ethanol were refluxed for three hours. The mixture was cooled to room temperature and filtered. The yellow product was washed with cold ethanol.

Synthesis of 4-chlorobenzylidene- 4'-alkanoyloxyaniline, nClAB

ClHAB (2 mmol) was initially dissolved in a minimum amount of DMF and added into a mixture of fatty acid (2 mmol) and DMAP (0.2 mmol) which has already been dissolved in dichloromethane (20 ml). DCC (2 mmol) in dichloromethane (5 mL) was added dropwise into the mixture upon stirring at 0°C for an hour, which was further stirred at room temperature for another three hours. Finally, the mixture was filtered and the excess solvent was removed from the filtrate by evaporation. The white product was recrystallized with ethanol until its transition temperature remained constant (Scheme 1). The percentage yield and analytical data of the title compounds are tabulated in Table 1.
EI-MS, IR, ^{1}H and ^{13}C NMR data of the representative compound 16ClAB are given as follows:

16ClAB: EI-MS (m/z, relative intensity): 231.0 (230) (100); 469.3 (469) (9); IR (KBr) (cm^{-1}): 2918, 2849 (CH_2 stretching), 1748 (C=O), 1618 (C=N), 1474 (C=C aromatic), 1210 (C-O); ^{1}H NMR (400 MHz, $CDCl_3$): δ/ ppm: 0.87 (t, 3H, *J* = 12.0 Hz, C$\underline{H}_3$-), 1.26-1.41 (m, 24H, CH_3-(C$\underline{H}_2$)$_{12}$-), 1.75 (q, 2H, *J* = 8.0 Hz, -C$\underline{H}_2$CH_2COO-), 2.58 (t, 2H, *J* = 16.0 Hz, -CH_2C$\underline{H}_2$COO-), 7.13 (d, 2H, *J* = 8.0 Hz, Ar-H), 7.24 (d, 2H, *J* = 8.0 Hz, Ar-H), 7.35 (d, 2H, *J* = 8.0 Hz, Ar-H), 7.91 (d, 2H, *J* = 8.0 Hz, Ar-H), 8.40 (s, 1H, C$\underline{H}$=N); ^{13}C NMR (75 MHz, $CDCl_3$), δ/ ppm: 14.10 (CH_3), 22.67, 24.80, 29.05, 29.08, 29.23, 29.34, 29.35, 29.58, 29.63, 29.66, 31.91, 34.41 (for methylene carbons), 122.08, 122.34, 129.08,129.22, 130.02, 131.52, 133.52, 150.34 (aromatic carbons), 159.38 (CH=N), 171.87 (COO).

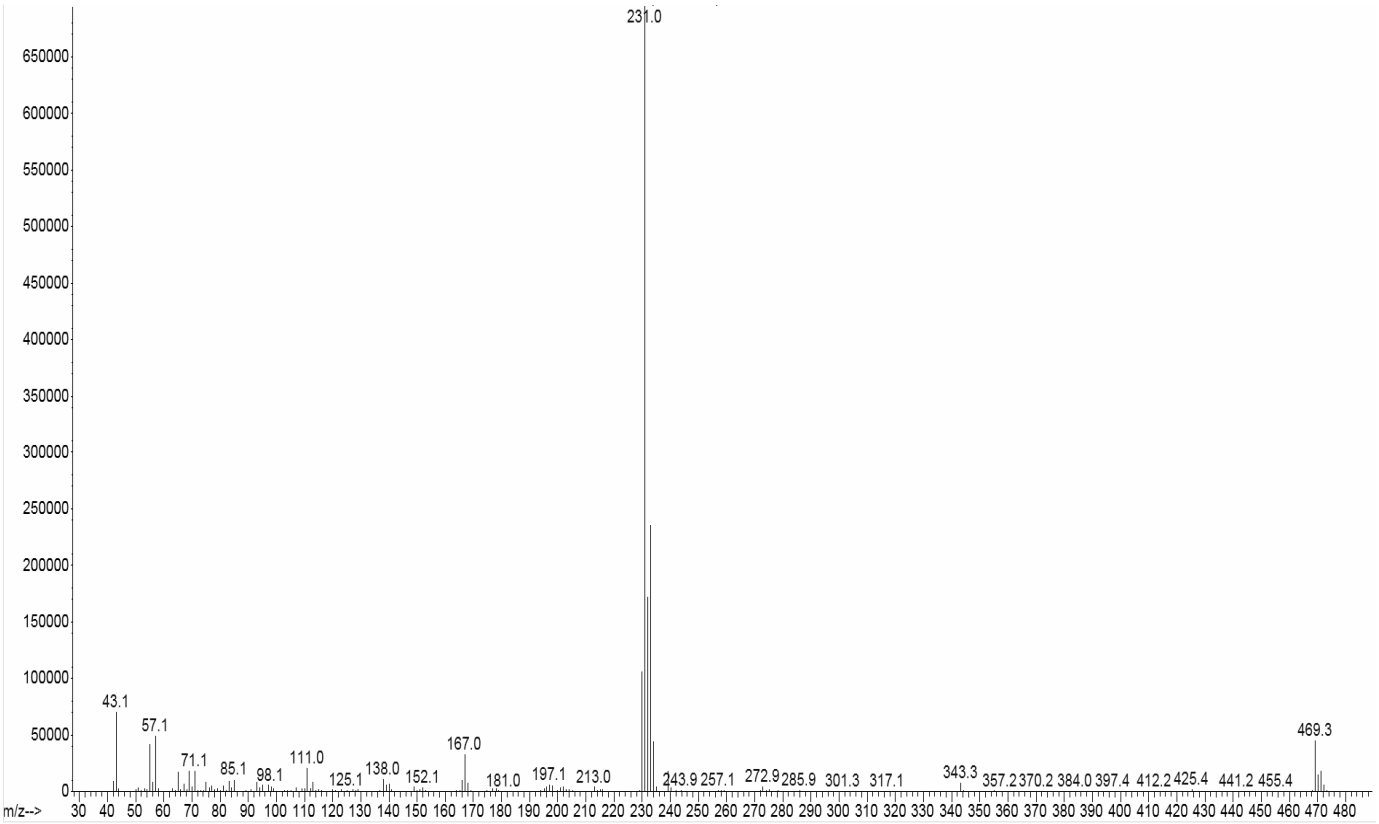

Figure 1. FTIR spectrum of 16ClAB.

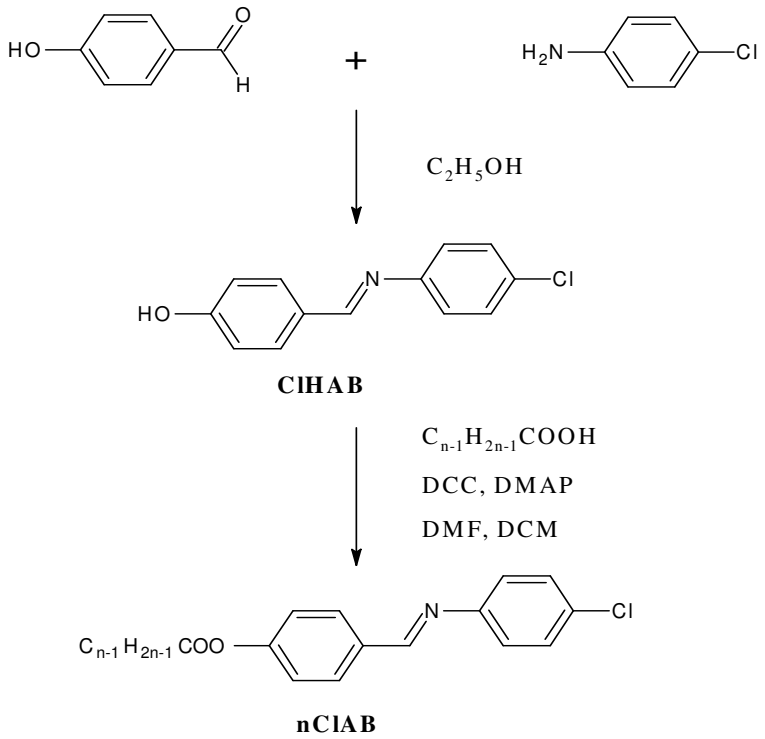

Scheme 1. Synthetic route of nClAB, where n= 2 - 8, 10, 12, 14, 16 and 18.

Table 1. Percentage yields and analytical data of nClAB.

Compound	Yield (%)	Formula	% Found (Calc.)		
			C	H	N
2ClAB	32	$C_{15}H_{12}ClNO_2$	65.93(65.82)	4.34(4.42)	5.09(5.12)
3ClAB	38	$C_{16}H_{14}ClNO_2$	66.89(66.79)	4.85(4.90)	4.79(4.87)
4ClAB	56	$C_{17}H_{16}ClNO_2$	67.77(67.66)	5.27(5.34)	4.59(4.64)
5ClAB	50	$C_{18}H_{18}ClNO_2$	68.41(68.46)	5.80(5.75)	4.40(4.44)
6ClAB	85	$C_{19}H_{20}ClNO_2$	69.08(69.19)	6.15(6.11)	4.32(4.25)
7ClAB	43	$C_{20}H_{22}ClNO_2$	69.90(69.86)	6.41(6.45)	3.99(4.07)
8ClAB	46	$C_{21}H_{24}ClNO_2$	70.57(70.48)	6.75(6.76)	3.82(3.91)
10ClAB	73	$C_{23}H_{28}ClNO_2$	71.65(71.58)	7.26(7.31)	3.53(3.63)
12ClAB	74	$C_{25}H_{32}ClNO_2$	72.42(72.53)	7.87(7.79)	3.43(3.38)
14ClAB	85	$C_{27}H_{36}ClNO_2$	73.50(73.36)	8.13(8.21)	3.10(3.17)
16ClAB	66	$C_{29}H_{40}ClNO_2$	74.00(74.09)	8.65(8.58)	3.00(2.98)
18ClAB	51	$C_{31}H_{44}ClNO_2$	74.90(74.74)	8.86(8.90)	2.73(2.81)

RESULTS AND DISCUSSION

Synthesis and spectral studies

Structure elucidation of compounds nClAB was ascertained by using elemental analysis, mass spectrometry and spectroscopic methods (FT-IR and NMR). The experimental and theoretical values obtained from the elemental analysis of nClAB (where n = 2 - 8, 10, 12, 14, 16 and 18) (Table 1) were in good agreement. The molecular ion peak at m/z = 469.3 in the mass spectrum of the representative compound 16ClAB (Figure 2) suggested that 16ClAB with a molecular formula of ($C_{29}H_{40}ClNO_2$) was successfully synthesized.

The ^{1}H NMR spectrum of 16ClAB (Figure 3) further supported its structure. The two triplets at δ = 0.87 ppm and δ = 2.58 ppm, were respectively ascribed to the methyl and methylene protons (-C$\underline{H_2}$COO-Ar), while the multiplet between δ = 1.26 - 1.41 ppm was assigned to the methylene protons of the long alkyl chain {-$(CH_2)_{12}$-}. The four distinct doublets between δ = 7.12 - 7.92 ppm were indicative of the aromatic protons. The singlet observed at the most downfield region, δ = 8.40 ppm, supported the presence of the imine linking group (Yeap et al., 2006c). The molecular structure of 16ClAB was further verified by using ^{13}C NMR spectroscopy (Figure 4). The peak at δ = 14.10 ppm was attributed to the methyl carbon while the peaks between δ = 22.67 - 34.41 ppm represented the methylene carbons of the long alkyl chain. The 12 carbons of the aromatic ring in 16ClAB resonated between δ = 122.08 - 150.34 ppm. The peak at δ = 159.38 ppm and δ = 171.87 ppm confirmed the presence of the azomethine carbon and the carbonyl group in the molecule.

Mesomorphic properties

5ClAB exhibited interesting thermotropic properties and its melting behavior was carefully monitored by POM during both heating and cooling scans. Optical photomicrographs of 5ClAB are shown in Figure 5 as the representative illustration. The results from the POM observation were verified by the DSC measurements. The transition temperatures, enthalpy changes, and phase sequences are summarized in Table 2. Phase identification was based on optical textures, and the magnitude of isotropization on enthalpies is consistent with the assignment of each mesophase type, using the classification systems reported by Sackmann and Demus (1966), and Gray and Goodby (1984).

Under POM, focal conic fan-shaped textures of a smectic A phase was observed during the cooling cycle (Figure 5a). Upon further cooling, the back of the fan-shaped domains developed a series of dark-lines, which is transitory in nature (Figure 5b) (Singh and Dunmur, 2002; Goodby and Gray, 1979). When further cooled, the bands expanded, met and eventually coalesce to produce a polygonal-like texture (Figure 5c) (Galewski and Coles, 1999). This phase is identified as a smectic B phase. This similar behavior was also reported for a closely-related compound, 4-butyloxybenzylidene-4-chloroaniline (Cozan et al., 2009).

X-ray diffraction studies

The XRD pattern of the representative compound 12ClAB is shown in Figure 6. In general, smectic, nematic and cholesteric structures exhibit a broad peak associated with a lateral packing at 2θ ≈ 16 - 21° in a wide-angle XRD curve. A sharp and strong peak at a low angle ($1^\circ < 2\theta < 6°$) in a small angle X-ray scattering curve can be observed for a smectic structure, however, not for nematic and cholesteric structures (Wang et al., 2007; Meng et al., 2008; Xiao et al., 2008). The XRD pattern of 12ClAB showed sharp reflection peaks at 2θ of 2.46° at

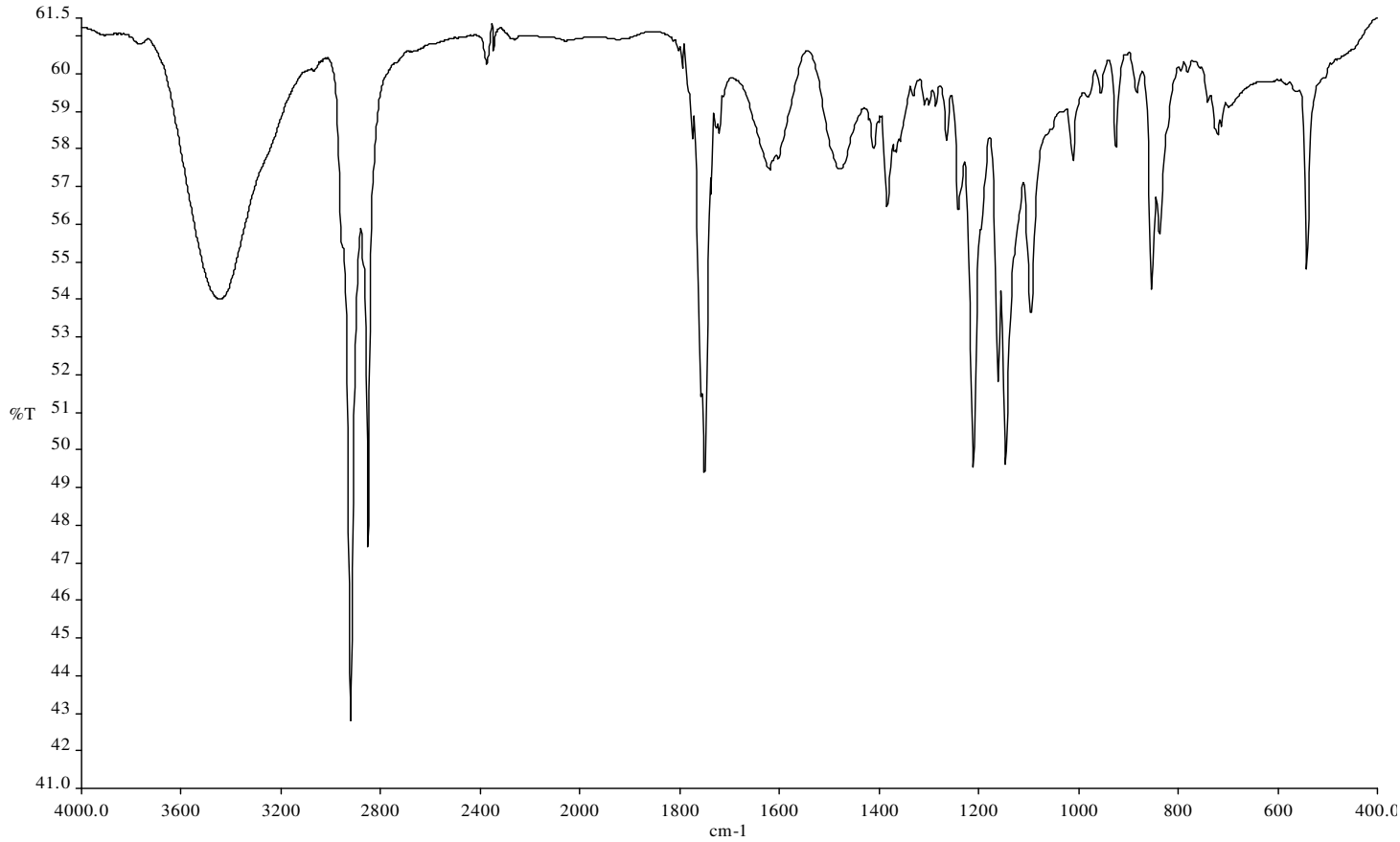

Figure 2. EI-MS spectrum of 16ClAB.

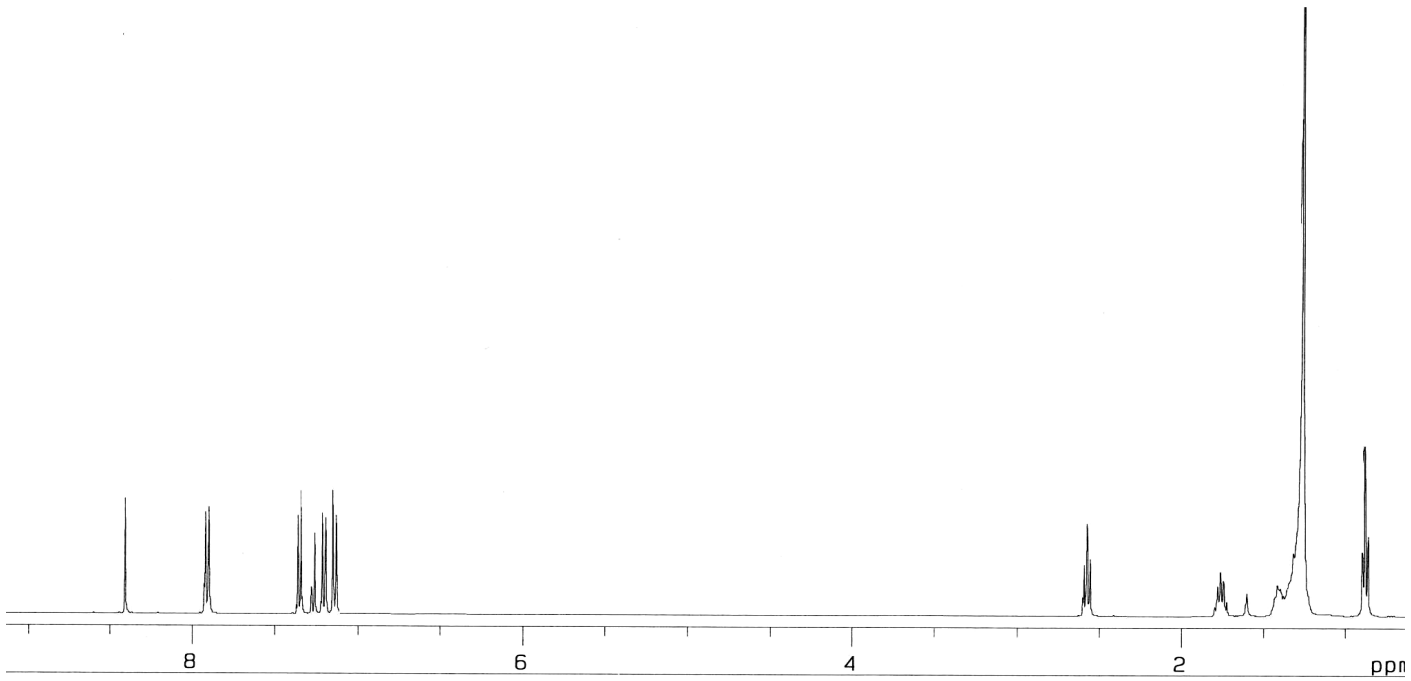

Figure 3. ^{1}H NMR Spectrum of 16ClAB.

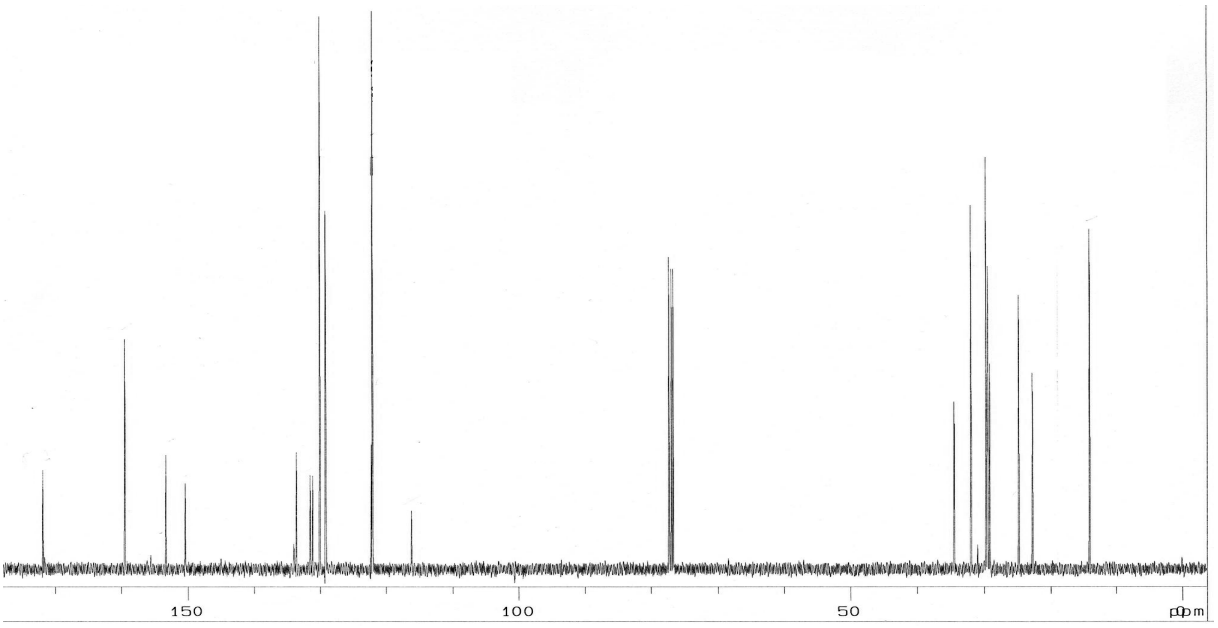

Figure 4. ^{13}C NMR Spectrum of 16ClAB.

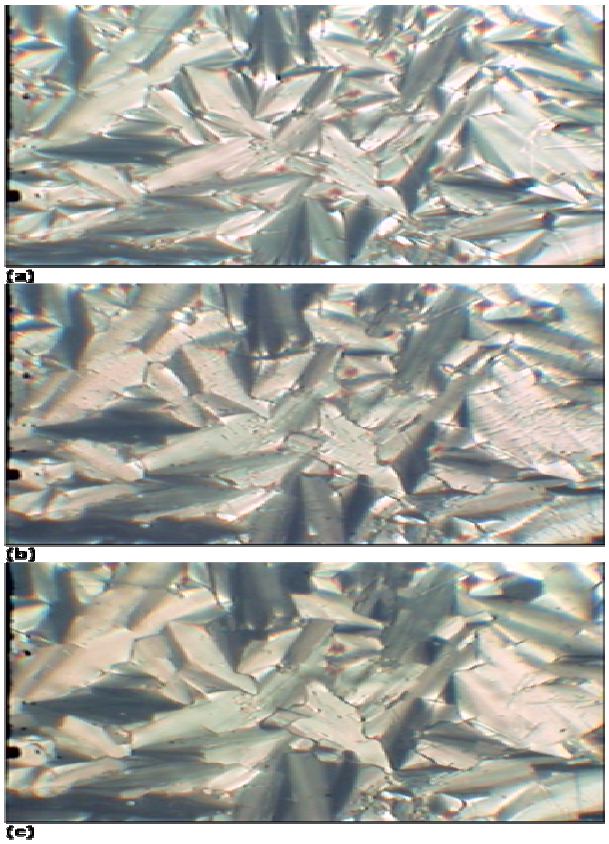

Figure 5. Optical photomicrographs of 5ClAB taken during the cooling cycle. (a) Optical photomicrograph showing fan-shaped textures of a SmA phase at 85.3℃ (b) Optical photomicrograph exhibiting transition bar at the SmA to SmB transition (at 80.2℃) (c) Optical photomicrograph displaying mosaic textures of a SmB phase at 65.8℃.

Table 2. Transition temperatures and associated enthalpy changes of nClAB upon heating and cooling scans.

Compound	Transition temperatures, ℃ (∆H, kJmol^{-1})
	Heating cooling
2ClAB	Cr 109.4 (26.3) I I 97.54 (26.11) Cr
3ClAB	Cr 92.7 (23.0) I I 66.0 (21.8) Cr
4ClAB	Cr 83.6 (35.5) I I 82.1(3.8) SmA 76.9 (3.6) SmB 13.1 (9.1) I
5ClAB	Cr 77.1 (29.8) SmB 82.5 (3.8) SmA 91.2 (6.7) I I 89.0 (6.9) SmA 80.5 (3.9) SmB (22.9) Cr
6ClAB	Cr 95.94 (46.32) I I 95.28 (6.44) SmA 77.50 (3.20) SmB (32.07) Cr
7ClAB	Cr 73.0 (14.0) SmB 83.9 (1.9) SmA 101.6 (3.9) I I 97.2 (3.9) SmA 78.2 (1.8) SmB 15.0 (7.9) Cr
8ClAB	Cr 84.0 (34.6) SmA 104.8 (6.7) I I 102.7 (6.9) SmA 80.2 (2.7) SmB 33.5 (27.8) Cr
10ClAB	Cr 83.4 (35.4) SmA 106.7 (8.0) I I 105.1 (8.2) SmA 79.9 (3.1) SmB 33.2 (28.5) Cr
12ClAB	Cr 86.3 (40.6) SmA 106.5 (8.0) I I 104.8 (8.1) SmA 78.0 (2.9) SmB 42.1 (33.9) Cr
14ClAB	Cr 89.8 (55.3) SmA 105.1 (9.2) I I 103.5 (9.1) SmA 75.8 (3.2) SmB 55.4 (49.5) Cr
16ClAB	Cr 92.8 (58.3) SmA 102.4 (8.6) I I 100.7 (9.4) SmA 72.8 (2.8) SmB 68.3 (53.7) Cr
18ClAB	Cr 94.5 (72.0) SmA 98.8 (8.9) I I 97.1 (10.1) SmA 76.7 (75.0) Cr

C r = Crystal; SmA = Smectic A; SmB = Smectic B; I = Isotropic liquid.

90℃, which corresponded to a smectic layer spacing. The *d*-layer spacing upon cooling from an isotropic liquid to a smectic A phase was 29.2Å whereas the molecular length obtained from the MM2 molecular calculation was 27.1Å. Since the *d/l* ratio was 1.08 (*d/l* = 1), this suggested that the smectic A phase for 12ClAB was of a monolayer arrangement (Liao et al., 2008). Therefore, it can be deduced that on average, the long molecular axis of 12ClAB pointed in one favorable direction with a small interaction coefficient.

Influence of alkyl chain length on mesomorphic properties

Representative DSC thermograms for nClAB (where n = 2, 5, 6, 8) upon heating and cooling are depicted in Figure 7. A plot of the transition temperatures against the number of carbons in the alkanoyloxy chain during theheating cycle are shown in Figure 8.

Out of the twelve compounds, the first two members (C2 and C3) did not possess mesomorphic properties.

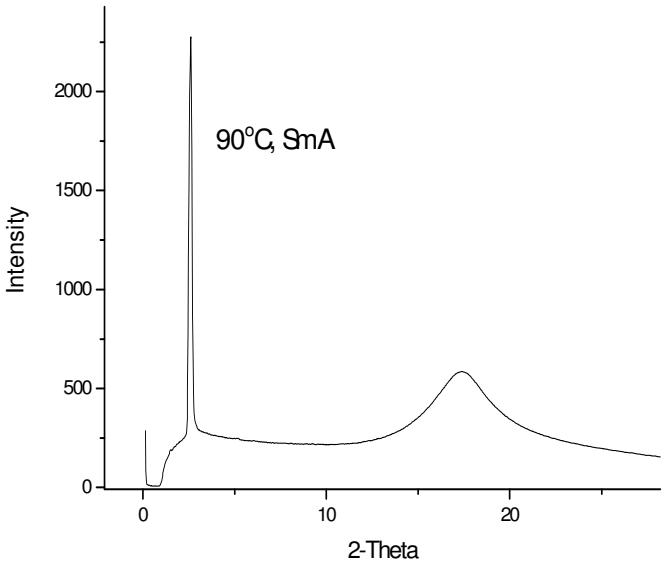

(a)

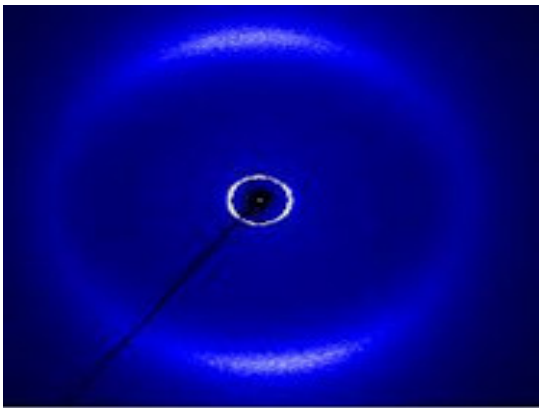

(b)

Figure 6. (a) XRD diffractogram at 90°C during the cooling cycle of 12ClAB (b) An X-ray diagram of a SmA phase of 12ClAB at 90°C upon cooling. The molecules are aligned in the magnetic field. The two sharp signals indicate a lamellar arrangement of the molecules.

These molecules with short alkanoyloxy chains are too rigid; therefore have high melting points, thus impeding their liquid crystal properties (Kumar et al., 2001). Once the length of the terminal chain is increased, the molecule becomes more flexible, hence promoting a monotropic mesophase in a particular compound. Therefore, the C4 and C6 members are monotropic smectogens whereby mesophases (SmA and SmB) were only observed during their cooling scans. As for the highest member of this series, the C18 member, and SmA phase was observed during both the heating and cooling cycles. Thus, C18 is an enantiotropic mesogen. C5 and C7 derivatives exhibited enantiotropic SmA and SmB phases. The rest of the members, C8 - C16 members exhibited enantiotropic SmA and monotropic SmB phases.

From the graph, the shortest member of the homologous series, C2, possessed the highest melting temperature (T_m = 109.4°C). The melting point decreased as the length of the chain increased to the C7 member (T_m = 73.0°C) with the exception of the C6 member. This resulted from the increase in the flexibility of the molecule owing to the longer alkyl chain. It is also common that the melting temperature increases from the medium chain member onwards following a decrease from the short to

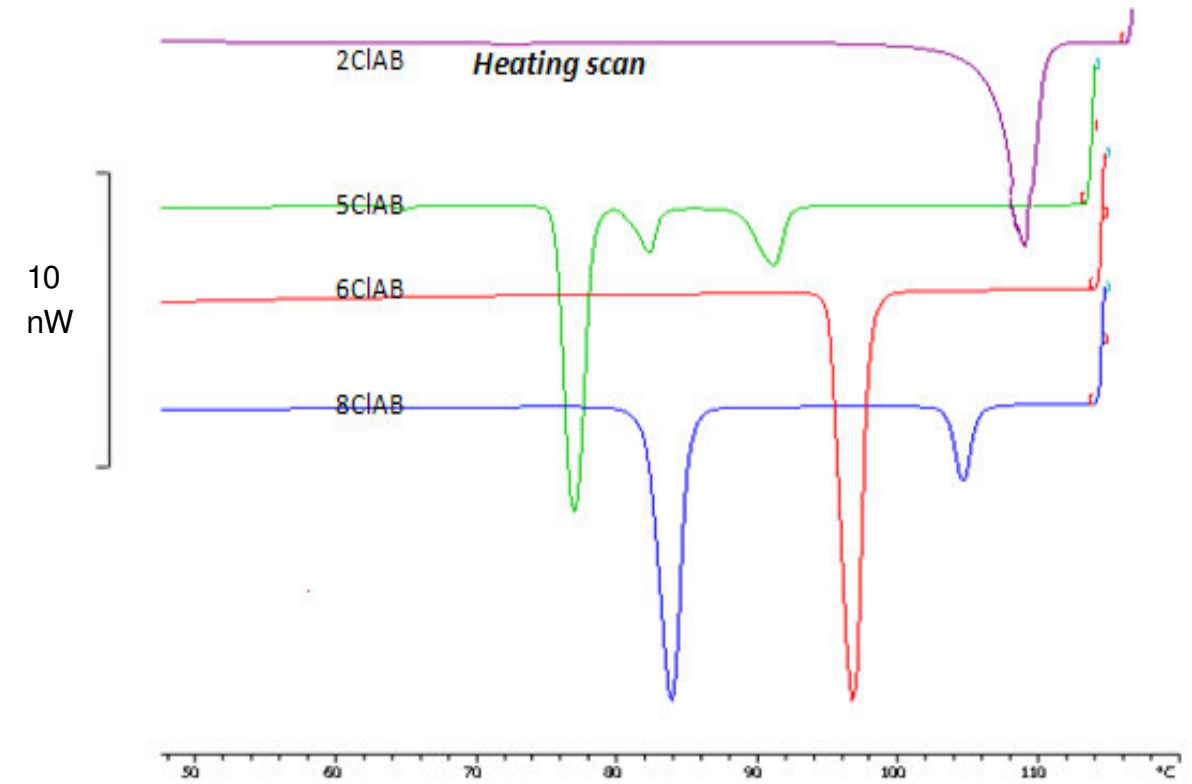

(a)

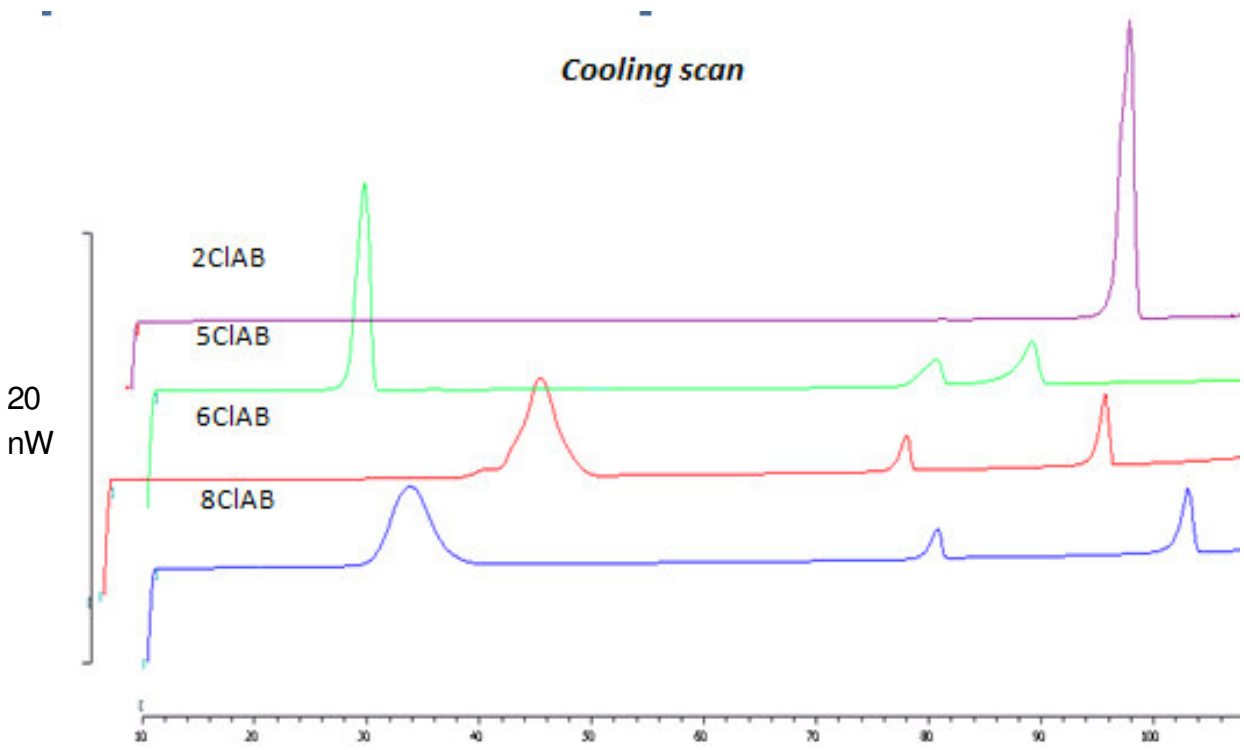

(b)

Figure 7. DSC thermograms of 2ClAB, 5ClAB, 6ClAB and 8ClAB during (a) heating and (b) cooling cycles.

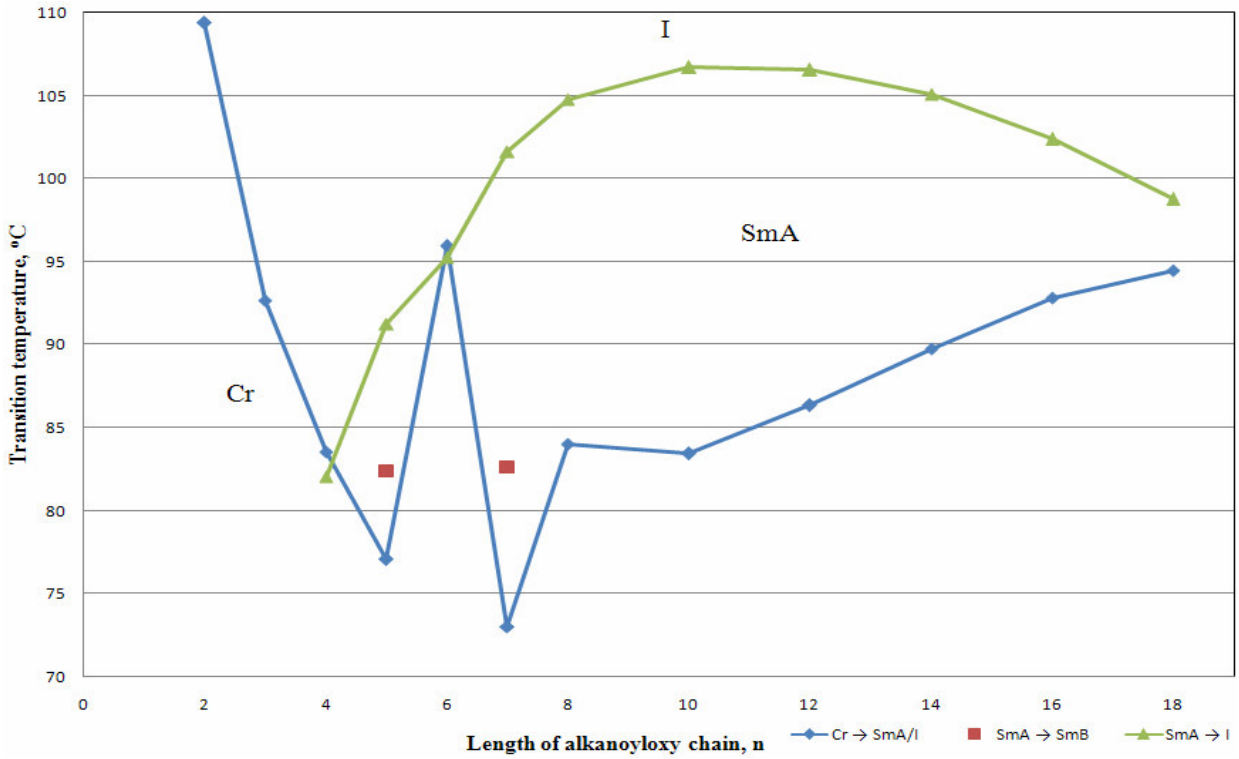

Figure 8. Plot of transition temperature versus the length of alkanoyloxy chain of nClAB during heating cycle.

Table 3. Comparison of mesomorphic behaviour of 8ClAB with structurally related compounds.

Compound	Structure and phase transition (°C)	Reference
8ClAB	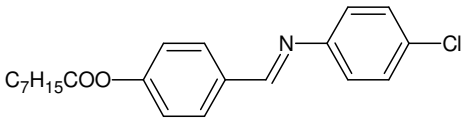 Cr (80.2)* SmB 84.0 SmA 104.8 I	[Present studies]
F-OAB	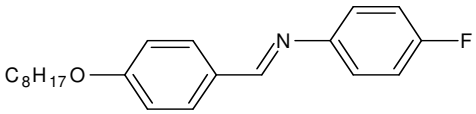 Cr (55.1)* SmB 62.2 SmA 65.2 I	(Gandolfo, 1988)
Cl-OAB	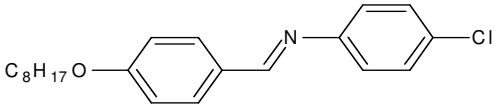 Cr 61.0 SmB 87.7 SmA 98.5 I	(Galewski, 1994)
Br-OAB	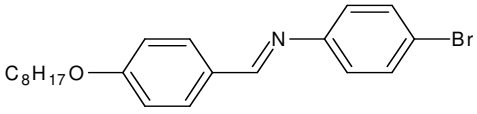 Cr 89.0 SmB 104.0 SmA 113.0 I	(Galewski, 1994)

( )* indicates monotropic phase.

the medium chain members (Kelker and Hatz, 1980). An increase in the melting temperature was also observed from the *n*-heptanoyloxy (T_m = 73.0°C) to the *n*-octadecanoyloxy (T_m = 94.5°C) derivative which could have been attributed to the increase in the Van der Waals attractive forces between the molecules (Gray, 1962).

The zig-zag pattern or the odd-even effect is observed in the melting temperatures of the lower members of the homologous series (C4, C5, C6, C7, and C8). As the series ascends from the C4 to the C8 member, the Cr-to-SmA/I transition temperatures attenuates consistently. The even members possessed high clearing temperatures compared to their odd member counterparts. Such attenuation of the melting temperatures has been observed in various homologous systems of liquid crystals (Kumar, 2001).

While the C4 to C10 members exhibited an increase in their transition temperatures during the SmA-to-I transition, the opposite was observed for the C10 to C18 members. The terminal intermolecular attractions play a role in determining the SmA-I transition temperatures, that is, the destruction of the smectic molecular order is determined by the fact that the terminal attractions become weaker, allowing partial interpenetration of the layers to occur more easily as the alkanoyloxy chains grow longer, in turn depressing the SmA-to-I transition temperatures (Prajapati and Bonde, 2009; Gray, 1962).

Structure-mesomorphic property relationships

Molecular structure of organic compounds and their liquid crystalline properties are closely related. Table 3 summarizes the transition temperatures, mesomorphic behavior and molecular structures of 8ClAB and structurally related compounds (Galewski, 1994; Gandolfo, 1988) reported in literature.

According to Table 3, 8ClAB showed an enantiotropic smectic A phase and monotropic smectic B phase, while Cl-OAB and Br-OAB showed enantiotropic smectic A and B phases. The dissimilarities in the mesophase properties were due to the difference in the linking groups (ester group in 8ClAB and ether group in Cl-OAB and Br-OAB) between the phenyl ring and the alkyl chain. The ether linking group provides greater linearity to molecules rather than the ester group, thus resulting in the more stable enantiotropic smectic B phase being observed in Cl-OAB and Br-OAB. In addition, 8ClAB possessed higher melting and clearing temperatures compared to Cl-OAB owing to the π-electrons associated with the carbonyl group which provides greater intermolecular interactions among molecules (Kumar, 2001).

Based on Table 3, it can be seen that the melting and transitions temperatures of 8ClAB are lower than those of Br-OAB. The bromine atom is larger than the chlorine atom and therefore more easily polarized due to the electrons on this atom which are loosely held and far from the nucleus (Solomons, 1994). Higher molecular polarizability contributed by the larger bromine atom led to higher phase stability in Br-OAB (Yeap et al., 2004). Based on the same reasoning, the smaller and the less polarizable fluorine atom in F-OAB resulted in it displaying melting and transition temperatures lower than that of 8ClAB.

ACKNOWLEDGEMENTS

The author (S.T. Ha) would like to thank Universiti Tunku Abdul Rahman (UTAR) for the UTAR Research Fund (Vote No. 6200/H02) and Postgraduate Bench Fee (Vote No. 6202/O05) which have funded this project. L.K. Ong would like to acknowledge UTAR for the award of the research assistantship. The powder XRD measurements were supported by beamline BL17A (charged by Dr. Jey-Jau Lee) of the National Synchrotron Radiation Research Center, Taiwan.

REFERENCES

Collings PJ, Hird M (1998). Introduction to Liquid Crystals Chemistry and Physics. Taylor and Francis Ltd. London.

Cozan V, Avadanei M, Perju E, Timpu D (2009). FTIR investigations of phase transitions in an asymmetric azomethine liquid crystal. Phase Transitions, 82(8): 607-619.

Dave JS, Menon M (2000). Azomesogens with heterocyclic moiety. Bull. Mater. Sci., 23: 237-238.

Eran BE, Nesrullajev A, Canli NY (2008). Characterization and investigation of the mesogenic, thermo-morphological and thermotropic properties of new chiral (S)-5-octyloxy-2-[{4-(2-methylbuthoxy)phenylimino(methyl)phenol liquid crystalline compound. Mat. Chem. Phys., 111: 555-558.

Galewski Z (1994). Liquid crystalline properties of 4-halogenobenzyline-4'-alkoxyanilines. Mol. Cryst. Liq. Cryst., 249: 43-49.

Galewski Z, Coles HJ (1999). Liquid crystalline properties and phase situations in 4-chlorobenzylidene-4'-alkylanilnes. J. Mol. Liq. 79: 77-87.

Gandolfo G, Grasso D, Beumi G, Torquatio G (1988). Phase transitions and structural studies of *p-n*-alkoxybenzylidene-*p'*-fluoro-anilines. IL Nuovo Cimento., 10: 1363-1371.

Goodby JW, Gray GW (1979). Tilted smectic B phase or smectic H phase?. J. *de Physique* 4: 363-370.

Gray GW (1962). Molecular structure and properties of liquid crystals. Academic Press, London.

Gray GW, Goodby JW (1984). Smectic Liquid Crystals: Textures and Structures, Leonard Hill.

Ha ST, Ong LK, Ong ST, Yeap GY, Wong JPW, Koh TM, Lin HC (2009a). Synthesis and mesomorphic properties of new Schiff base esters with different alkyl chains. Chin. Chem. Lett., 20: 767-780.

Ha ST, Yeap GY, Boey PL (2009b). Synthesis and liquid crystalline properties of new Schiff bases N-[4-(4-n-alkanoyloxybenzoyloxy)benzylidene]-4-cyano-, 4-hydroxy-, 4-thio-and 4-nitroanilines. Aust. J. Basic Appl. Sci. 3(4): 3417-3422.

Kelker H, Hatz R (1980). Handbook of Liquid Crystals. Verlag Chemie, Florida.

Kelker H, Scheurle B (1969). A liquid crystalline (nematic) phase with a particularly low solidification point. Angew. Chem. Int. Edn. 8: 884-885.

Kumar S (2001). Liquid Crystals: Experimental Study of Physical Properties and Phase Transitions. Cambridge University Press, Cambridge.

Liao CC, Wang CS, Sheu HS, Lai CK (2008). Symmetrical dimer liquid crystals derived from benzoxazoles. Tetrahedron., 64: 7977-7985.

Meng FB, Gao YM, Lian J, Zhang BY, Zhang FZ (2008). Synthesis and characterization of side-chain liquid-crystalline polysiloxanes

containing fluorinated units. Colloid Polym. Sci. 286: 873-879.
Parra M, Vergara J, Zuniga C, Soto E, Sierra T, Serrano JL (2004). New chiral Schiff's bases with a 1,3,4-thiadizole ring in the mesogenic core: synthesis, mesomorphic and ferroelectric properties. Liq. Cryst., 32: 457-462.
Petrov VF, Duan M, Okamoto H, Mu J, Shimizu Y, Takenaka S (2001). Halogenation in achiral liquid crystals: terminal and linking substitutions. Liq. Cryst., 28: 387-410.
Prajapati AK, Bonde NL (2009). Mesogenic benzothiazole derivatives with a polar nitro substituent. Mol. Cryst. Liq. Cryst., 501: 72-85.
Prajapati AK, Varia CC (2008). Azomesogens with polar chloro, nitro and phenolic –OH substituents. Liq. Cryst. 35: 1271-1277.
Sackmann H, Demus D (1966). The polymorphism of liquid crystals. Mol. Cryst. Liq. Cryst., 2: 81-102.
Sakagami S, Nakamizo M (1980). Liquid crystalline properties of N-(alkoxybenzylidene) -4-halogenoanilines. Bull. Chem. Soc. Jpn., 53: 265-266.
Singh S, Dunmur DA (2002). Liquid Crystals: Fundamentals. World Scientific Publishing Co. Pte. Ltd. London.
Solomons TWG (1994). Fundamentals of organic chemistry. John Wiley and Sons, New York.
Vora R, Prajapati AK and Kevat J (2001). Effect of terminal branching on mesomorphism. Mol. Cryst. Liq. Cryst., 357: 229-237.
Wang Y, Zhang BY, He XZ, Wang JW (2007). Side-chain cholesteric liquid crystalline polymers containing menthol and cholesterol-synthesis and characterization. Colloid Polym. Sci. 285: 1077-1084.
Xiao W, Zhang B, Cong Y (2008). Preparation and characterization of side-chain liquid crystalline polymers containing chenodeoxycholic acid residue. Colloid Polym. Sci., 286: 267-274.
Yeap GY, Ha ST, Boey PL, Mahmood WAK, Ito MM, Youhei Y (2006a). Synthesis and characterization of some new mesogenic Schiff base esters N-[4-(4-n-hexadecanoyloxybenzoyloxy)benzylidene]-4-substitued anilines. Mol. Cryst. Liq. Cryst., 452: 73-90.
Yeap GY, Ha ST, Lim PL, Boey PL, Ito MM, Sanehisa S, Vill V (2006b). Nematic and smectic A phases in ortho-hydroxy-para-hexadecanoyloxybenzylidene-para-substituted anilines. Mol. Cryst. Liq. Cryst., 452: 63-72.
Yeap GY, Ha ST., Boey PL, Ito MM, Sanehisa S, Youhei Y (2006c). Synthesis, physical and mesomorphic properties of schiff base esters containing ortho-,meta- and para-substituents in benzylidene-4'-alkanoyloxyanilines. Liq. Cryst., 33: 205-211.
Yeap GY, Ha ST, Lim PL, Boey PL, Mahmood WAK, Ito MM, Sanehisa S (2004). Synthesis and mesomorphic properties of Schiff base esters ortho-hydroxy-para-alkyloxybenzylidene-para-substituted anilines. Mol. Cryst. Liq. Cryst., 423: 73-84.
Yuksel F, Atilla D, Ahsen V (2007). Synthesis and characterization of liquid crystalline unsymmetrically substituted phthalocyanines. Polyhedron, 26: 4551-4556.
Zhang BY, Meng FB, Tian M, Xiao WQ (2005). Side-chain liquid-crystalline polysiloxanes containing ionic mesogens and cholesterol ester groups. React. Funct. Polym., 66: 551-558.